Cement and Concrete Research 40 (2010) 340–346

Contents lists available at ScienceDirect

Cement and Concrete Research

journal homepage: http://ees.elsevier.com/CEMCON/default.asp

# Nonlinear ultrasonic evaluation of load effects on discontinuities in concrete

P. Antonaci [a], C.L.E. Bruno [a,*], P.G. Bocca [a], M. Scalerandi [b], A.S. Gliozzi [b]

[a] Structural and Geotechnical Engineering Department, Politecnico di Torino, Corso Duca degli Abruzzi 24, 10129 Torino, Italy
[b] Physics Department, Politecnico di Torino, Corso Duca degli Abruzzi 24, 10129 Torino, Italy

ARTICLE INFO

*Article history:*
Received 16 June 2009
Accepted 18 September 2009

*Keywords:*
Characterization (B)
Mechanical properties (C)
Microcracking (B)
Degradation (C)
Concrete (E)

ABSTRACT

The presence of discontinuity surfaces in concrete structures, i.e. two or more layers in contact, may be an existing situation with evident relapses on damage formation and progression. Differences occur depending on the type of discontinuity, which could be a thin weaker layer or a pre-existing crack. The behavior of pre-existing interfaces is here studied by means of the Scaling Subtraction Method, a Nonlinear Ultrasonic Non-Destructive Technique, that revealed to be effective in describing the mechanical evolution of concrete samples with discontinuity surfaces under the effects of compressive loads.



## 1. Introduction

Discontinuity surfaces such as joints in large concrete structures are often indicated as weak areas where damage may begin to propagate from. Its progression appears in the form of increasing crack density [1] and/or growing crack openings [2,3], depending on the geometry of the structure considered and on loading conditions. In particular, damage mechanisms seem to differ depending on the nature of the discontinuity, i.e. an existing crack [4] or a weaker layer [5–7]. Both kinds of discontinuities are very common in concrete structures, often with severe consequences on their structural performances and durability.

Macroscopic cracks may be produced by unexpected loads, seismic events, subsidence phenomena, etc. [4]. Damage progression may easily take its starting point from the weak area thus created and its severity mainly depends on the crack size, opening and location.

Discontinuities in the form of a weaker material layer are also frequent in concrete structures. One only needs to think of interfaces between multiple castings [5] or patch repair works [6,7]: if no proper precautions are adopted, a typical deleterious consequence could be the formation of a thin low-quality layer at the interface between fresh and seasoned material. Again, the layer itself or the region close to it [8] can easily fail at load levels lower than expected.

In this paper, both a "crack-like discontinuity" and a "low-quality layer discontinuity" have been experimentally studied. Accordingly, two types of laboratory specimens have been produced: the first was made of two piled concrete cubes (the interface between the two cubes roughly simulating a macroscopic crack) and the second was made of two similar concrete cubes piled one on the other with the interposition of a thin layer of low-quality cement paste. A specific damage process was induced by means of compressive uniaxial load steps and its progression was analyzed by means of the Scaling Subtraction Method (SSM) [9,10], a Nonlinear Ultrasonic Non-Destructive Technique.

The same way as other well-established nonlinear ultrasonic methods, the SSM is concerned with the detection of nonlinear terms in the elastic response of a solid to a linear ultrasonic wave excitation. Among them, successive harmonic components [11–13], nonlinear attenuation [14], amplitude dependent phase delay [15], resonance frequency shift [16,17], modulated frequencies [18,19], multi-mode resonance spectroscopy [20] etc., are universally considered to be related to the presence of micro-cracks and/or to a deterioration of the material properties. Differently than most of the other filtering-based techniques [21], however, the SSM presents the advantage that no parameters are needed for the analysis and that the quality of the results is less affected by the increase of the distance between transducers and nonlinear scatterers [22]. In addition, as it will be shown in the following, the SSM makes it possible to account for nonlinear terms at the fundamental frequency, which in general have a relevant magnitude and allow to conduct experiments in a narrow frequency band, with a significant improvement of the signal-to-noise ratio.

For these reasons, and in consideration of its easy experimental implementation and complete non-destructiveness, the SSM turns out to be particularly attractive in view of its potential application for the on-site assessment of existing structures. Its effectiveness has already been demonstrated in evaluating damage occurrence in homogeneous concrete and mortar samples with experimental evidence [10].

Here we show that the SSM (discussed in Section 2) is a suitable technique to study the evolution of damage in proximity of

* Corresponding author.
*E-mail addresses:* paola.antonaci@polito.it (P. Antonaci), caterina.bruno@polito.it (C.L.E. Bruno), pietro.bocca@polito.it (P.G. Bocca), marco.scalerandi@infm.polito.it (M. Scalerandi), antonio.gliozzi@polito.it (A.S. Gliozzi).

0008-8846/$ – see front matter © 2009 Elsevier Ltd. All rights reserved.
doi:10.1016/j.cemconres.2009.09.014

discontinuity surfaces. Indeed, we prove it to be sensitive to very small changes in the nonlinearity of the sample and hence to the related damage evolution steps (Section 3.4). Furthermore, the validity of the approach is independent on the arrangement of the transducers, i.e. both direct and indirect transmission modes work equally well. Elsewhere, it has also been shown that the relative distance between damaged area and transducers is not a relevant issue [22]. Finally, we show that the evolution of nonlinearity at low load levels is different for the cases of a "low-quality layer discontinuity" and for a "crack-like discontinuity", while their behavior is very similar at large load levels (Section 4).

## 2. The Scaling Subtraction Method

The presence of elastic nonlinear portions of material in damaged media breaks the proportionality between input signals (i.e. the electrical signals, measured in Volts, proportional to a mechanical excitation, usually expressed as stresses) and output signals (i.e. the electrical signals proportional to the dynamic deformations in the medium due to the ultrasonic propagating wave, usually expressed as strains). The superposition principle is no longer applicable and the elastic response to an impinging ultrasonic wave contains nonlinear terms which show a dependence on the amplitude of the injected wave. The break of proportionality can be retraced to three main mechanisms [9,23]:

1. Nonlinear losses of elastic energy.
2. Redistribution of energy among the various generated frequencies.
3. Dependence on amplitude of the phase of the response.

The Scaling Subtraction Method (SSM) takes advantage of such break of proportionality in order to extract the signature of damage in an ultrasonic signal. In a very general treatment, when a nonlinear medium is excited by a sinusoidal monochromatic wave of amplitude $A$ and frequency $\omega_0$, the signal recorded after propagating through the sample can be written in terms of a Fourier Series:

$$v_A(t) = \sum_{n=1}^{\infty} B_n(A)\left[\cos(n\omega_0 t + \phi_n(A))\right]. \quad (1)$$

Notice that both the amplitude coefficients $B_n$ and phases $\phi_n$ have a dependence on the amplitude $A$ of the excitation. Nonlinear features are extracted from the signal in the form of Eq. (1) by means of a simple subtraction with a linear reference signal $v_{\mathrm{ref}}(t)$.

To define $v_{\mathrm{ref}}(t)$, it is reasonable to assume that when the sample is excited by a sufficiently low amplitude $A_{\mathrm{lin}}$, nonlinear terms are negligible and the recorded signal, which can be experimentally measured, can be considered as the linear elastic response of the specimen:

$$v_{\mathrm{lin}}(t) = B_1(A\to 0)\cos(\omega_0 t + \phi_1). \quad (2)$$

Thus, the linear reference signal ($v_{\mathrm{ref}}$) at a higher amplitude $A = kA_{\mathrm{lin}}$ ($k \gg 1$) can be constructed by applying the proportionality principle, valid if the system was linear. The elastic response expected from an equivalent linear sample would have been:

$$v_{\mathrm{ref}}(t) = kv_{\mathrm{lin}}(t) \neq v_A(t) \quad (3)$$

where $v_A$ is the actual nonlinear signal at high amplitude, i.e. the one measured in the nonlinear sample.

Once the reference signal is defined by simply subtracting the linear reference of Eq. (3) to the nonlinear measured signal (which is in the form of Eq. (1)) one obtains an electric signal containing only the nonlinear response of the specimen, which will be denoted as the SSM signal:

$$w_A(t) = v_A(t) - v_{\mathrm{ref}}(t). \quad (4)$$

The SSM signal depends on the amplitude ($A$) of the injected wave. We stress here that the nonlinear signature in the SSM signal $w_a(t)$ takes into account not only higher order harmonics and sidebands (which may be present depending on the experiment), but also the nonlinear contributions at the fundamental frequency, such as nonlinear attenuation and phase shift, both normally cancelled by a filtering technique.

A quantitative parameter able to represent the nonlinear signature can be defined. In particular, the SSM indicator was introduced as the "energy" of the SSM signal $w_A(t)$:

$$\theta(A) = \frac{1}{T}\int_0^T w_A^2(t)dt \quad (5)$$

where $T$ is a proper time window. Likewise, a variable that represents the "energy" of the recorded output was defined as:

$$x(A) = \frac{1}{T}\int_0^T v_A^2(t)dt \quad (6)$$

Here, the term "energy" is used in a signal processing context [24]. The energy in the usual physical meaning can be derived using the electrical load of the acquisition set-up, but that goes beyond the scope of this paper.

## 3. Experimental set-up

### 3.1. Materials and samples

Four test pieces were produced, each one obtained by piling up two concrete cubes measuring 10 cm on each side. Two kinds of discontinuities were obtained at the interface between the cubes. Two of the test pieces, which in the following will be denoted as specimens A1 and A2, were joined using a thin layer of cement paste. The two other test pieces, which in the following will be denoted as specimens B1 and B2, were laid one on the other, with cubes casting surfaces in direct contact. All cubes were produced using a concrete mix with CEM II A-L 42.5 R cement, ordinary aggregates (max. size = 16 mm) and a water to cement ratio equal to 0.74, with no admixtures. Their age at the date of testing was approximately six months.

The mechanical characteristics of the concrete were preliminarily evaluated by means of mono-axial static compression tests, that resulted in a compressive strength of 24 N/mm$^2$ (240 kN maximum load). The longitudinal wave speed in the cube was measured to be $v_t = 3850$ m/s and the density of the cubes was $\rho = 2330$ kg/m$^3$.

### 3.2. Testing equipment

The following ultrasonic testing equipment was used:

- Four identical piezoelectric transducers with a diameter of 40 mm and resonance frequency of 55.5 kHz. One was used as emitting source and the remaining three as receivers.
- An arbitrary waveform generator, used to drive the emitting source, forcing it to vibrate according to a burst law of 10 sinusoidal cycles at a frequency of 55.5 kHz. The amplitudes of the input signals thus generated were controlled in order to be progressively increasing.
- A high voltage linear amplifier.
- A data acquisition unit, equipped with an oscilloscope for real-time data visualization. Signals were recorded with a sampling rate of 10 MSa/s, according to Nyquist's theorem.

Linearity of the testing apparatus in working conditions was carefully verified in order to avoid any possible spurious effect that could alter the experimental data. Transducers were attached to the faces of each specimen through a thin layer of phenyl salicylate, whose linearity was preliminarily verified using a reference linear

sample. Tests were conducted simultaneously in direct transmission mode (i.e. transducers attached to two opposite faces of the specimen) and in indirect transmission mode (i.e. transducers attached to the same face of the specimen). For a more detailed explanation of the experimental set-up see Fig. 1. Repeatability of measurements was also verified.

Different load levels were applied to the specimens thus equipped by means of a 250 kN servo-controlled Mechanical Testing System (MTS), working under controlled loading velocity.

### 3.3. Experimental procedure

The same mechanical and ultrasonic testing protocol was followed for the four test pieces. Specimens were loaded by means of a uniaxial compressive force, with increasing intensity until rupture occurred. At selected load levels, ultrasonic measurements were conducted keeping the specimen under constant load in the MTS frame. Experiments with ultrasonic measurements performed on unloaded samples are in progress to analyze the reversibility of damage processes.

Each set of measurements, i.e. one for each load level, was performed according to the SSM procedure described in Section 2. In particular, the amplitude of the excitation was varied between 1 and 200 V peak to peak, after amplification, for a total number of 27 steps. Notice that albeit samples were excited by means of short sinusoidal bursts, the theoretical conclusions of Section 2 still remain valid, with slight modifications of the formalism.

The 27 recorded signals $v_i(t)$ $(i=1\ldots27)$ were analyzed as discussed in Section 2. The linear signal $v_{\mathrm{lin}}$ was chosen, for each load level, so as to assure signals to be out of noise level: $v_{\mathrm{lin}}$ was chosen as the first output signal with a peak to peak amplitude larger than 25 mV. The SSM indicator $\theta$ was calculated and plotted vs. $x$ (see Eqs. (5) and (6) for the definitions). The faster the increase of $\theta$ as a function of $x$ is, the stronger the nonlinearity of the sample is expected to be. Note that, for a perfectly linear sample, $\theta$ is identically zero (except for noise effects) for any value of $x$.

### 3.4. Efficiency of the SSM

With reference to the specimen A1, experimental output signals at different input amplitudes and corresponding to diverse load levels are shown in Fig. 2, in order to prove the efficiency of the SSM. When low load levels are applied, which is the case of the first and second rows (representing signals recorded at 5 kN and 35 kN loads respectively), signals do not show a significant change of their shape with the increase of amplitude. Slight modifications of the shape as a function of the injected amplitude can be appreciated in signals recorded at larger loads (last row, corresponding to 75 kN). The shape dependence on amplitude can be here an indication of nonlinearity, as it will be pointed out in the application of the SSM (Section 4).

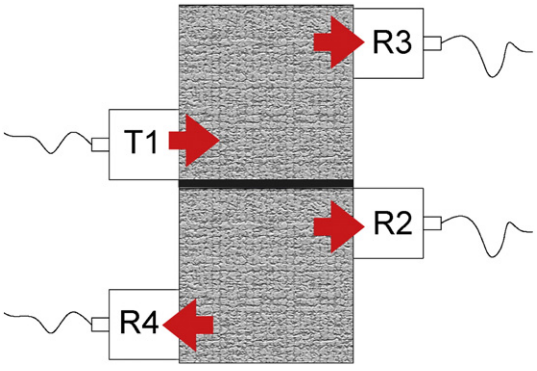


**Fig. 1.** Experimental set-up: arrangement of transducers on the sample. Transducer T1 was used as emitter while transducers R2, R3 and R4 were used as receivers. Notice that R2 and R3 receive signals in direct transmission mode while R4 receives signals in indirect transmission mode. Also, the direct path to R2 and R4 crosses the discontinuity, while that for R3 does not.

We would like to remark that the FFT analysis of all signals reported in Fig. 2 (including those at larger excitation energy) does not enlighten the presence of higher order harmonics, since they fall below noise level, probably also due to the use of narrow band transducers. Accordingly, traditional nonlinear methods concerned with the detection of harmonics, such as Nonlinear Elastic Wave Spectroscopy [25], are expected to be inefficient in highlighting the presence of nonlinearity in our experiment.

A variation of the signal shape is appreciable when comparing signals at different load levels but corresponding to the same injected amplitude (read Fig. 2 per columns). Such an effect can be interpreted as an indication of the change of the elastic properties of the medium due to the application of the mechanical load and can be thus related to damage. On the other hand, this is not an absolute measurement of damage and the same effect of variation of the shape could be ascribed to other effects as well, e.g. to a change in the coupling quality or in the transducers arrangement, which could be eventually detached and re-attached due to experimental reasons. The nonlinearity indication provided by the SSM is instead an absolute measure of nonlinearity, since the reference signal is contained in the measurement itself.

For the same load levels and amplitudes, the SSM signals were reported in Fig. 3: the SSM approach acts as a magnifying glass, enabling to observe the variations of the waveforms with increasing excitation amplitude. The SSM signals shown here have been calculated according to the procedure described in Section 2 and normalized to the output amplitude of the corresponding $v_i(t)$ signals. Notice that the magnitude of the SSM signals significantly increases with the increase of the injected amplitude, thus showing that nonlinearity increases with the increase of the injected amplitude. Despite the increase of attenuation given by the increase of damage (read Fig. 2 by columns), the normalization of the SSM signals to their corresponding $v_i(t)$ allows to observe that the nonlinear response increases with the increase of the applied load and hence with the increase of damage (read Fig. 3 by columns).

## 4. Results

In this Section we will discuss a few experimental results to show that:

- The SSM is sensitive to small changes in the nonlinearity of the sample.
- The validity of the approach is independent on the arrangement of the transducers, i.e. both direct and indirect transmission modes work equally well.
- The evolution of the nonlinearity at low load levels is different for the cases of a low-quality layer and for a crack-like discontinuity, while the behavior is very similar at large load levels.

The two discussed cases will be analyzed separately in the following.

### 4.1. Low-quality layer discontinuity

With reference to specimen A1, signals recorded at each load step have been analyzed by means of the Scaling Subtraction Method. Fig. 4 shows the $\theta$ parameter versus the energy of the recorded output signal ($x$) for a few selected load steps; experimental data (symbols) have been fitted by means of a power law (solid lines):

$$\theta = a\left(\frac{x}{x_{\mathrm{ref}}}\right)^{b} x_{\mathrm{ref}} \tag{7}$$

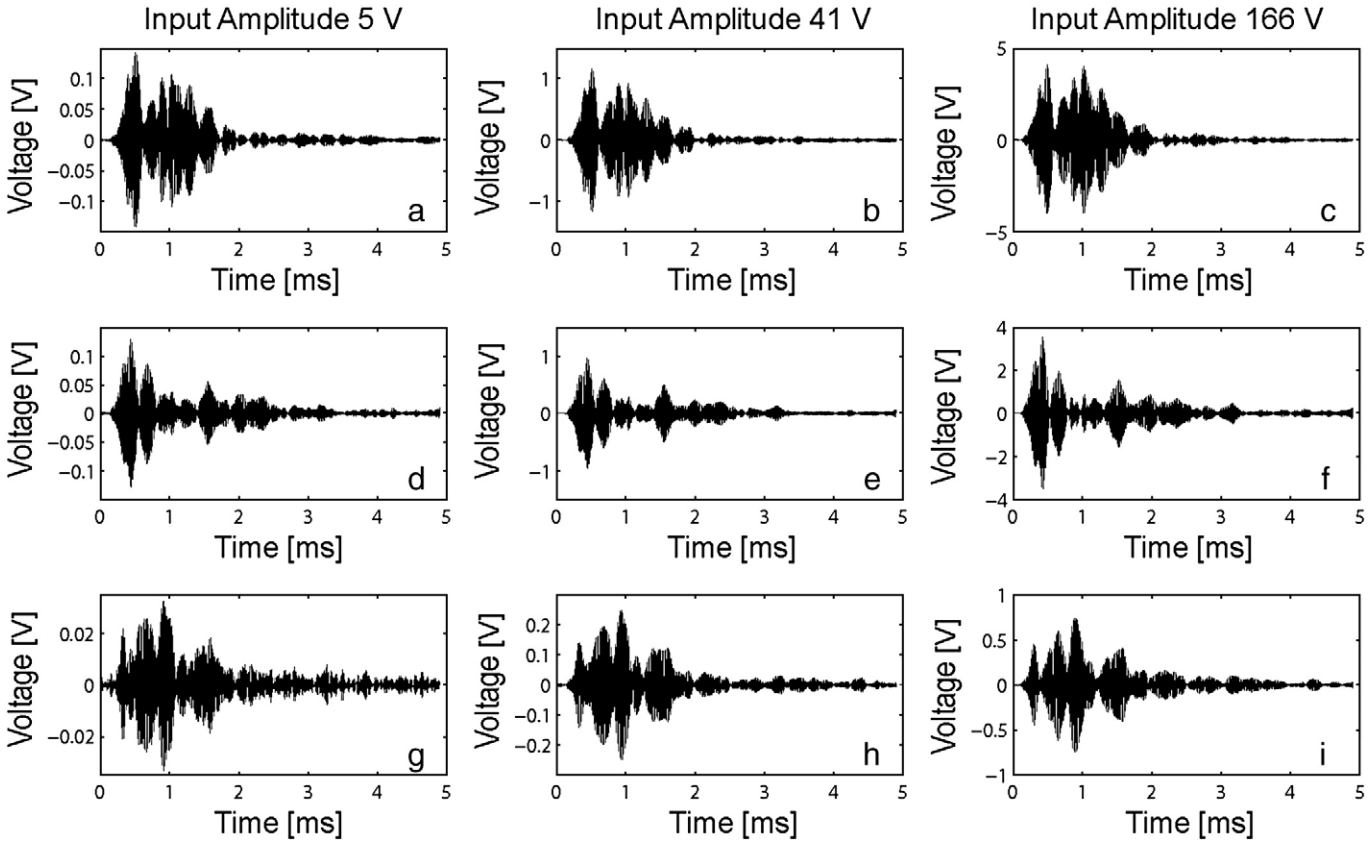


**Fig. 2.** Experimental signals recorded on specimen A1 ("low-quality layer discontinuity"): columns correspond to 5, 41 and 166 V of input amplitudes, while rows correspond to 5, 35 and 75 kN load levels. Notice that, for low load levels (5 and 35 kN) the shape of the waveforms does not show relevant changes among signals at the same fixed load. A variation of the shape as function of the injected amplitude can be appreciated for higher load levels (75 kN, last row).

with $x_{ref}=A_{lin}^2$, where $A_{lin}$ is the lowest excitation amplitude. See Eqs. (5) and (6) for the definition of $\theta$ and $x$.

The analysis reported in Fig. 4 refers to signals recorded by transducer R4. The nonlinearity does not immediately increase with the rise of load and for low compressions a compaction effect is observable. Indeed, the slope of the curves decreases until about 10 kN load level is reached (less than 10% of the failure load). A slight increase of nonlinearity can be appreciated from 10 to 50 kN. A clear rise of $\theta$ is reached for higher load levels when the specimen is close to collapse. Indeed, fractures close to the bonding layer are evident at 90 kN and their propagation can be visually followed, resulting in macroscopic fractures. For higher load levels, portions of cement were spalled from the cubes.

A clearer view of the evolution of nonlinearity, and thus of damage progression, can be appreciated by analyzing the nonlinear indicator as a function of the applied load at a fixed value of the input energy. In Fig. 5 the value of $\theta_0=\theta(x_0)$, extrapolated from the fitting function, is reported versus load. The value of $x_0$ was fixed at 0.5 $V^2$ and no qualitative changes occurred when varying this choice.

According to the trend of nonlinearity expressed in Fig. 5, three main stages in the evolution of the specimen properties can be envisaged:

1. For low compressive loads (0 to 20 kN) a rearrangement of the internal structure, with micro-structures collapsing and pores closing down, occurs. It is possible that also early damage in the discontinuity takes place, but the decrease in nonlinearity indicates that it is a minor effect if compared to compaction in the cubes and in the layer too.
2. Higher load levels (20 to 70 kN, about 50% of the failure load) give rise to a small increase of nonlinearity and reasonably early damage occurs in the discontinuity.
3. Late damage occurs from 70 kN to rupture (failure occurred at 150 kN). Here, a noticeable increase of nonlinearity indicates damage in the cubes. Notice that Fig. 5 shows a change in the slope: nonlinearity (damage) increases faster and faster with load.

Fig. 6 reports the same analysis of $\theta_0$ versus load on signals recorded by all three transducers. Even if differences in magnitude are visible, no relevant changes occur for receivers R2 (direct transmission) and R4 (indirect transmission): from the equivalence of the results obtained in the two configurations it follows that the SSM may as well be applied in direct or indirect transmission modes.

Slight differences can be appreciated in the analysis of data recorded by receiver R3 (direct transmission and not crossing the discontinuity), where the distinction between intermediate and late stages of damage evolution is less evident. This configuration of transducers is indeed less sensitive to the damage of the discontinuity and most of the nonlinear information contained in the signals recorded by R3 comes from reflections.

### 4.2. Crack-like discontinuity

The same experiments (with the same experimental set-up) conducted on specimens A1 and A2 have been performed on specimens with a "crack-like discontinuity", i.e. two piled concrete cubes (specimens B1 and B2), which could be a rough approximation of the case of a pre-existing crack.

The analysis of the nonlinear parameter $\theta_0$ versus load for specimens B1 and B2 shows differences in damage occurrence. In particular Fig. 7, which refers to specimen B1, shows a dissimilarity in the low loading stage (0 to 20 kN) and in the evolution of damage.

Regarding the first stage (low load levels), the space between the cubes acts here as a clapping element: when no load is applied the two

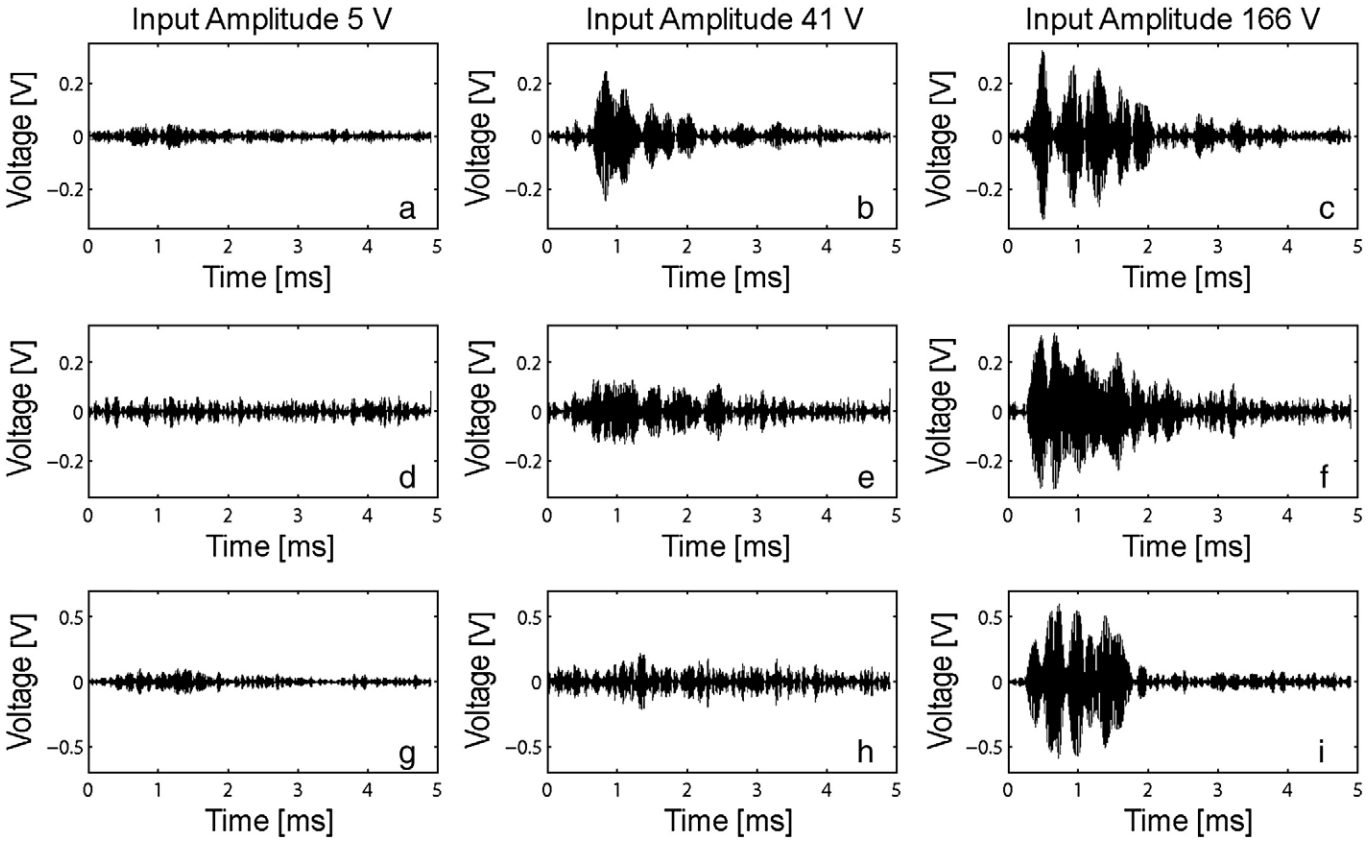


**Fig. 3.** SSM signals calculated using Eq. (4) from waveforms of Fig. 2: columns correspond to 5, 41 and 166 V of input amplitudes, while rows correspond to 5, 35 and 75 kN load levels. Notice that the magnitude of the signals significantly increases with the increase of the injected amplitude. SSM signals have been normalized to the corresponding recorded output. As load increases (fix a column and scan through rows) the SSM signals show an increase of amplitude, thus showing an increase of nonlinear content.

surfaces are free to clap one against the other, generating strong nonlinear contributions in the elastic response of the system (much higher than for sample A1). A very low load is sufficient to close the surfaces together and prevent them from clapping, with a consequent drastic decrease of nonlinearity. The further decrease of $\theta_0$ is due, in our opinion, to compaction of concrete. Notice that only receivers R2 and R4 capture this trend, while receiver R3 (direct transmission mode, not crossing the interface) does not show any decrease of nonlinearity. Indeed, we assume that as long as the "crack-like discontinuity" is open almost none of the components of the signal recorded by receiver R3 has crossed the discontinuity in its travelling path and only few nonlinear components are present in the recorded signal. For the same reason, when low loads are applied, signals recorded by receiver R3 have higher amplitudes than signals recorded by receivers R2 and R4, which are highly attenuated when crossing the interface.

For what concerns the damage evolution (intermediate and high load levels), notice that the three stages previously observed (see Figs. 5 and 6) are not evident here. Indeed, the intermediate stage is

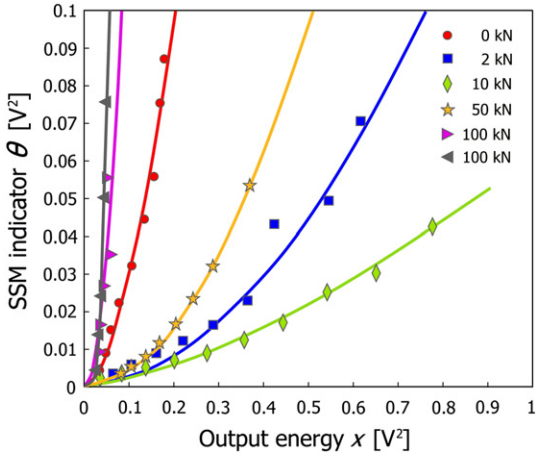


**Fig. 4.** SSM indicator $\theta$ versus energy of the output signal for sample A1 ("low-quality layer" discontinuity). The analysis corresponds to receiver R4. A decrease in nonlinearity is observable for loads up to 10 kN. For larger loads, the SSM indicator begins to rise. Nonlinearity has a relevant increase when 100 kN are reached and fracture in the bulk begins. Solid lines represent a power law fitting. Failure occurred at 150 kN.

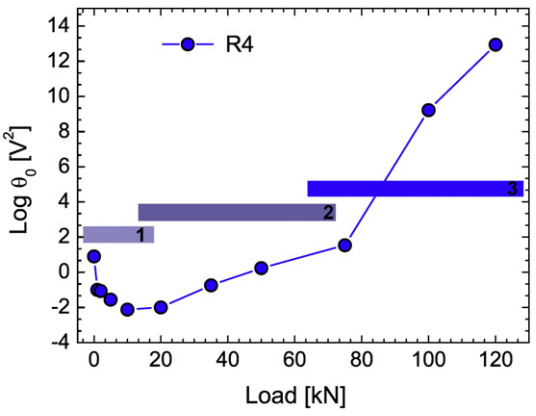


**Fig. 5.** SSM indicator at a fixed output energy value ($\theta_0 = \theta(x_0)$) as a function of load for sample A1: analysis of data recorded by receiver R4. The value of $\theta_0$ has been extracted from the fitting function at a fixed output energy value $x_0 = 0.5\ V^2$. Three stages in the evolution of the nonlinearity can be defined: compaction, formation of early damage and formation of late (macroscopic) damage. Solid lines only serve as a guide to the eye.

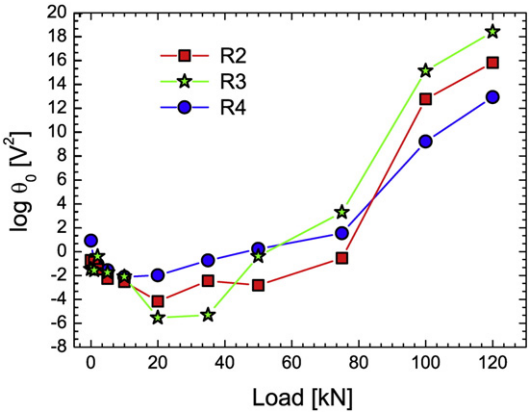


**Fig. 6.** SSM indicator at a fixed output energy value ($\theta_0 = \theta(x_0)$) as a function of load for sample A1: analysis of results given by the three receivers (R2, R3 and R4). The value of $\theta_0$ has been extracted from the fitting function (power law) at a fixed output energy value $x_0 = 0.5\ V^2$. Although signals recorded in different configurations are different in amplitude, no qualitative differences are appreciable when comparing data recorded from different receivers. Solid lines only serve as a guide to the eye.

not evident and only bulk damage occurs since the interface is a "crack-like discontinuity".

### 4.3. Discussion

The results reported in the previous Subsections allow us to make a few considerations about the efficiency of the SSM procedure and the mechanisms of damage evolution in concrete in proximity of discontinuity surfaces.

For what concerns the SSM procedure, it appears that it works equally well in both direct transmission mode (source and receiver on opposite faces of the sample) and indirect transmission mode (source and receiver on the same face of the sample), as it can be seen in the results for R2 and R4 reported in Figs. 6 and 7. The advantages for "in situ" applications are evident.

On the contrary, considering the location of the discontinuity with respect to transducers, we observe that the sensitivity decreases when operating in reflection rather than in transmission modes. Indeed, the signal at transducer R3 is mostly dominated by reflections at the discontinuity and the SSM method, in this case, is not sensitive enough to appreciate damage at the interface. This is valid for both the "low-quality layer" and the "crack-like" discontinuities.

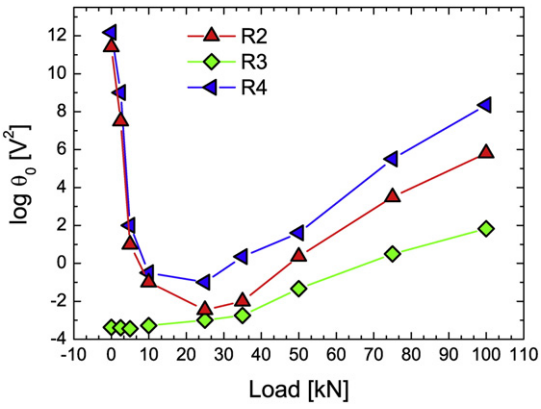


**Fig. 7.** SSM indicator at a fixed output energy value ($\theta_0 = \theta(x_0)$) as a function of load for sample B1: analysis of data recorded by the three receivers. The value of $\theta_0$ has been extracted from the fitting function (power law) at a fixed output energy value $x_0 = 0.5\ V^2$. Apart from low loads, where different receivers highlight the different response of the specimen, the behavior of the "crack-like" discontinuity is qualitatively similar to that of sample A1 reported in Fig. 6. Solid lines only serve as a guide to the eye.

Also, the sensitivity to low loads (see Fig. 8) is different for R3 with respect to the other transducers. Indeed, results for samples A2 and B2 confirm the behavior observed for the A1 and B1 samples (Figs. 6 and 7) and the nonlinear response for receiver R3 is much lower than for the other two receivers in both cases.

As for the mechanisms of damage evolution, they are different for the two kinds of discontinuities, since for samples B1 and B2 there is no evidence of the intermediate stage observed for samples A1 and A2. This is actually to be expected, since only the weak layer can be damaged independently from the bulk, thus revealing an "active" role. This is confirmed by the fact that R3 is not sensitive to the second damage state also in the case of a "low-quality layer" discontinuity (see Fig. 6).

After the stage in which damage occurs at the interface only, the two discontinuities behave similarly till rupture. It is interesting to remark that the failure load is approximately the same for the four samples (about 150 kN) and much lower than the one expected for an equivalent sample without interfaces (the latter being expected to be slightly lower than the single cube failure load: 250 kN). However, it is important to observe a variation in the onset of bulk damage. In the "crack-like" discontinuity it appears already at around 30% of the failure load, while it begins at about 50% of the failure load in the case of a "low-quality layer" discontinuity.

It is also interesting to observe that some analogies can be found between nonlinearity and the changes in permeability [26–28] or the progression of Acoustic Emission (AE) phenomena induced by compressive loads [29–31]. Linking these three complementary observations may help to shed light on the physical processes which play a role in damage formation.

Although all these techniques provide information about crack opening/closure and damage development, it has to be pointed out, however, that significant differences characterize them in terms of potential applications for the purposes of material assessment. For instance, AE-based techniques are particularly suitable to be used as passive monitoring techniques, while the SSM is expected to be applicable as an active inspection methodology, since nonlinearities can be stimulated and eventually detected whenever required through active external US excitation.

## 5. Conclusion

In this paper we have shown that the evolution of damage due to quasi-static compressive loads applied to concrete samples with discontinuity surfaces cannot be easily detected using traditional methods. On the contrary, the Scaling Subtraction Method has revealed to be an efficient Nonlinear Non-Destructive Technique to

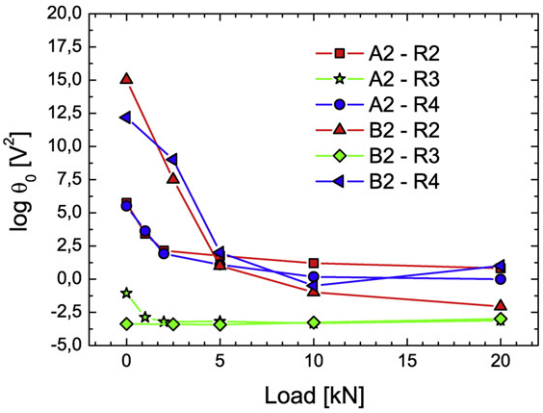


**Fig. 8.** Comparison of the trend of the SSM indicator at a fixed output energy value ($\theta_0 = \theta(x_0)$) for the "low-quality layer" discontinuity (sample A2) and the "crack-like" interface (sample B2). $\theta_0$ is reported versus load levels, for low loads only. Solid lines only serve as a guide to the eye.

evaluate the mechanical evolution related to damage in the samples. In particular, its ability to highlight the dependence of a recorded waveform on the input energy has borne out to be sensitive to the evolution of the elastic properties of the specimens.

The method, while extremely requiring in terms of linearity of the acquisition system, does not need accurate electronic devices or broad-band transducers. Furthermore, since the signal-to-noise ratio is improved due to the use of the fundamental frequency component of the signal, the closeness of the transducers to the damaged area is not as relevant as for other nonlinear techniques.

The method has proven to be very efficient in discriminating between "crack-like discontinuities" and "low-quality layer discontinuities", which manifest a different nonlinear behavior at low load levels. Further applications of the SSM method can be envisaged, e.g. to study the effect and extent of Alkali Silica Reaction [32], microcracks induced by concrete shrinkage [33] and chemical degradation [34] in laboratory specimens. We expect this method to be efficient also in such applications and further improvement should be obtained, from a quantitative point of view, based on the investigation about the possible existence of critical thresholds.

Finally, with regard to the assessment of full-scale structures, the SSM appears to be promising, albeit realistic applications still need the solution of several technical problems. In particular, issues regard the proper choice of the excitation frequency in order to overcome difficulties related to material attenuation.

## Acknowledgements

Financial support by the Italian Ministry of Education, University and Research (Grant no. 20077ESJAP003) is gratefully acknowledged.

## References

[1] B. Paliwal, K.T. Ramesh, An interacting micro-crack damage model for failure of brittle materials under compression, J. Mech. Phys. Solids 56 (3) (2008) 896–923.
[2] J.C. Galvez, J. Cervenka, D.A. Cendonc, V. Saouma, A discrete crack approach to normal/shear cracking of concrete, Cem. Concr. Res. 32 (10) (2002) 1567–1585.
[3] J. Zhang, V.C. Li, Simulation of crack propagation in fiber-reinforced concrete by fracture mechanics, Cem. Concr. Res. 34 (2) (2004) 333–339.
[4] F. Barpi, S. Valente, Modeling water penetration at dam-foundation joint, Eng. Fract. Mech. 75 (3–4) (2008) 629–642.
[5] B. Djazmati, J.A. Pincheira, Shear stiffness and strength of horizontal construction joints, ACI Struct. J. 101 (4) (2004) 484–493.
[6] A. Sharif, M.K. Rahman, A.S. Al-Gahtani, M. Hameeduddin, Behaviour of patch repair of axially loaded reinforced concrete beams, Cem. Concr. Compos. 28 (8) (2006) 734–741.
[7] P.S. Mangat, F.J. O'Flaherty, Influence of elastic modulus on stress redistribution and cracking in repair patches, Cem. Concr. Res. 30 (1) (2000) 125–136.
[8] P. Antonaci, C.L.E. Bruno, A.S. Gliozzi, M. Scalerandi, Evolution of damage in proximity of discontinuities in concrete, Int. J. Sol. Struct. (submitted for publication, 2009).
[9] M. Scalerandi, A.S. Gliozzi, C.L.E. Bruno, D. Masera, P. Bocca, A scaling method to enhance detection of a nonlinear elastic response, Appl. Phys. Lett. 92 (10) (2008) 101912(1–3).
[10] C.L.E. Bruno, A.S. Gliozzi, M. Scalerandi, P. Antonaci, Analysis of elastic nonlinearity using the Scaling Subtraction Method, Phys. Rev. B 79 (6) (2009) 064108(1–13).
[11] K. van den Abeele, J. De Vissche, Damage assessment in reinforced concrete using spectral and temporal nonlinear vibration techniques, Cem. Concr. Res. 30 (9) (2000) 1453–1464.
[12] P. Antonaci, P. Bocca, D. Masera, N. Pugno, M. Scalerandi, F. Sellone, A novel ultrasonic technique to detect damage evolution in quasi-brittle materials, Key Eng. Mat. 347 (2007) 633–638.
[13] I. Solodov, G. Busse, Nonlinear air-coupled emission: the signature to reveal and image microdamage in solid materials, Appl. Phys. Lett. 91 (25) (2007) 251910.
[14] P.A. Johnson, A. Sutin, Slow dynamics and anomalous nonlinear fast dynamics in diverse solids, J. Acoust. Soc. Am. 117 (1) (2005) 124–130.
[15] F. Vander Meulen, S. Dos Santos, L. Haumesser, O. Bou Matar, Contact phase modulation method for acoustic nonlinear parameter measurement in solid, Ultrasonics 42 (1–9) (2004) 1061–1065.
[16] K. van den Abeele, J. Carmeliet, J.A. TenCate, P.A. Johnson, Nonlinear Elastic Wave Spectroscopy (NEWS) techniques to discern material damage, Part II: Single-mode nonlinear resonance acoustic spectroscopy, Res. Nondestruct. Eval. 12 (1) (2000) 31–42.
[17] M. Bentahar, H. El Aqra, R. El Guerjouma, M. Griffa, M. Scalerandi, Hysteretic elasticity in damaged concrete: quantitative analysis of slow and fast dynamics, Phys. Rev B 73 (1) (2006) 014116.
[18] K. Warnemuende, H.C. Wu, Actively modulated acoustic nondestructive evaluation of concrete, Cem. Concr. Res. 34 (4) (2004) 563–570.
[19] J.C. Lacouture, P.A. Johnson, F. Cohen-Tenoudji, Study of critical behavior in concrete during curing by application of dynamic linear and nonlinear means, J. Acoust. Soc. Am. 113 (3) (2003) 1325–1332.
[20] A.S. Gliozzi, M. Nobili, M. Scalerandi, Modelling localized nonlinear damage and analysis of its influence on resonance frequencies, J. Phys. D: Appl. Phys. 39 (2006) 3895–3903.
[21] T.J. Ulrich, P.A. Johnson, M. Muller, D. Mitton, M. Talmant, P. Laugier, Application of nonlinear dynamics to monitoring progressive fatigue damage in human cortical bone, Appl. Phys. Lett. 91 (21) (2007) 213901(1–3).
[22] M. Scalerandi, A.S. Gliozzi, C.L.E. Bruno, K. van den Abeele, Nonlinear acoustic time reversal imaging using the scaling subtraction method, J. Phys. D: Appl. Phys 41 (21) (2008) 215404(1–10).
[23] L.A. Ostrovsky, P.A. Johnson, Dynamic nonlinear elasticity in geomaterials, Riv. Nuovo Cim. 24 (7) (2001) 1–46.
[24] J.O. Smith, Mathematics of the Discrete Fourier Transform (DFT) with Audio Applications, II editionW3K Publishing, 2007.
[25] K. van den Abeele, P.A. Johnson, A. Sutin, Nonlinear Elastic Wave Spectroscopy (NEWS) techniques to discern material damage. Part I: Nonlinear Wave Modulation Spectroscopy (NWMS), Res. Nondestr. Eval. 12 (1) (2000) 17–30.
[26] M. Saito, H. Ishimori, Chloride permeability of concrete under static and repeated compressive loading, Cem. Concr. Res. 25 (4) (1995) 803–808.
[27] V. Picandet, A. Khelidj, H. Bellegou, Crack effects on gas and water permeability of concretes, Cem. Concr. Res. 39 (6) (2009) 537–547.
[28] V. Picandet, A. Khelidj, G. Bastian, Effect of axial compressive damage on gas permeability of ordinary and high-performance concrete, Cem. Concr. Res. 31 (11) (2001) 1525–1532.
[29] H. Elaqra, N. Godin, G. Peix, G. Fantozzi, Damage evolution analysis in mortar, during compressive loading using acoustic emission and X-ray tomography: effects of the sand/cement ratio, Cem. Concr. Res. 37 (5) (2007) 703–713.
[30] M. Ohtsu, H. Watanabe, Quantitative damage estimation of concrete by acoustic emission, Constr. Build. Mat. 15 (5–6) (2001) 217–224.
[31] T. Suzuki, M. Ohtsu, Quantitative damage evaluation of structural concrete by a compression test based on AE rate process analysis, Constr. Build. Mat. 18 (3) (2004) 197–202.
[32] X. Mo, B. Fournier, Investigation of structural properties associated with alkali-silica reaction by means of macro- and micro-structural analysis, Mater. Charact. 58 (2) (2007) 179–189.
[33] P. Lura, B. Pease, G. Mazzotta, F. Rajabipour, J. Weiss, Influence of shrinkage-reducing admixtures on the development of plastic shrinkage cracks, ACI Mater. J. 104 (2) (2007) 187–194.
[34] M.A. Bader, Performance of concrete in a coastal environment, Cem. Concr. Comp. 25 (4–5) (2003) 539–548.